

Thermopower in Si-Ge Alloy Nanowire

Kasala Suresha

Department of Physics, Government First Grade College, MCC B Block, Davanagere – 577 004, India

Received: 26 Feb 2023; Received in revised form: 22 Mar 2023; Accepted: 31 Mar 2023; Available online: 08 Apr 2023

©2022 The Author(s). Published by AI Publications. This is an open access article under the CC BY license

<https://creativecommons.org/licenses/by/4.0/>

Abstract— In this article, we studied the past and existing research in nanowire (NW) especially based on SiGe NWs. The basic Thermoelectric (TE) principles and theories are introduced and the factors that may influence the TE performance of SiGe NWs are discussed. The superiority of the group IV material-based NWs as TE materials are detailed with feasible structures while their fabrication methods and TE measurements are also reviewed. The existing SiGe NW are discussed for their potential applications and the feasible applications are illustrated. Finally, the variation of parameter TE on Temperature and carrier concentration is discussed and compare theoretically with the available experimental data.

Keywords— Thermopower, Si-Ge alloy, Nanowire, electron diffusion, phonon drag

I. INTRODUCTION

Researchers have long been focused on locating new carbon-free and environmentally friendly energy alternatives [1]. Most of the energy that we consume is wasted in the form of heat. Thermal energy scavenging or harvesting, achieved by a thermoelectric generator (TEG), has the strength of stable components, high reliability, long service life, no maintenance, and direct energy conversion [2]. Because of this, TEGs have become the most promising device with core materials for harvesting wasted heat, as a result of a temperature difference.

In recent years, different research groups have fabricated micro-thermoelectric generators (μ TEGs) which are much smaller than the traditional TEGs [3]. Micro-thermoelectric generators fabrication apply the NW techniques commonly used in CMOS technology or micro electromechanical systems (MEMS) [4].

Recently, scientists have experimented with many nanostructured materials to make a high performance μ TEG. Besides the elementary substances like bismuth [5] and silicon [6], a large number of composite materials, including clathrates [7], skutterudites [8], metal oxides [9], tellurides [10], and inter-metallics [11], have been investigated for their TE performance. A key issue for this TE research is to find a high-performance TE material with low thermal conductivity and high electric conductivity. More possible solutions have been put forward and verified; one of the most promising materials is silicon. Silicon and its Group IV binary or ternary alloys

have potential to be used to form a TEG in commercial application for several reasons. They would be Si-based CMOS technology compatible, the source of the Group IV materials is much cheaper than the traditional TE materials, and rather than poisonous materials like Bi_2Te_3 , the Group IV materials are environment-friendly and safe for civil use.

However, despite its high thermal conductivity, Si bulk is unideal for TEG. Because of the popularization of Si electronics, researches on Si thermoelectric devices are expanding [12]. Two promising roads have been researched to improve the TE performance. The former is the alloying effect, which introduces other extended group IV materials with the same lattice structure, the typical one being SiGe. Compared to pristine Si, the experiment results show a distinct decrease in thermal conductivity. Interest has also been given to nanostructures, with quantum confinement applied. The development in nanoengineering makes it possible for nanostructures in Si-based TEG. The low-dimensional structures exhibit a significantly reduced lattice thermal conductivity compared to their bulk counterparts owing to the enhanced phonon scattering at the interfaces, and nanowires (NWs) have been proven with high ZT [13].

Nowadays, with further research, Si-based CMOS technology shows its potential to make a high-performance μ TEG [14]. Meanwhile, the scaling down in the fabrication of CMOS makes it possible to grow extremely thin Si and SiGe NWs. In general, two approaches have

been adopted for the fabrication of different NWs: top-down or bottom-up [15]. In most of the research we have investigated, the bottom-up approach is preferred with the popular vapor liquid- solid chemical vapor deposition (VLS-CVD) used [16]; others are achieved using the top-down approach with an etching process, for example, metal-assisted wet chemical etching (MaCE) or reactive ion etching (RIE) [17]. Some relevant measurements of the TE properties have also been developed during the study of NWs [18]. The typical methods for the Seebeck coefficient measure are mesoscopic or micro fabricated suspended devices and thermocouples. The micro fabricated suspended devices have also been used in the measurement of thermal conductivity. The other methods commonly used are the 3&methods and scanning thermal microscope (SThM) technique [19]. Micro-thermoelectric generators has a great variety of potential applications, including business electronics, bio-medical devices, and internet of things (IoT) devices. Internet of things devices are the most promising prospect for the μ TEG with a steady μ WmWlevel energy supply [20].

II. Theory

It is assumed that, the temperature is high enough to maintain an equipartition regime of electron-phonon interaction, in which the number of occupation of the phonon modes contributing to carrier diffusion and phonon drag effect. The most efficient Thermoelectrics have been heavily doped semiconductors because the Pauli principle restricts the heat carrying electrons to within $k_B T$ of the Fermi level for metals. Semiconductors have a lower density of carriers, leading to larger thermopower values implying that the electrical and thermal conductivities are somewhat decoupled. Thermal conductivity can be reduced by using bulk semiconductors of high atomic weight, which decreases the speed of sound. However, this strategy has not yet produced materials with figure of merit greater than unity. For metal or highly doped semiconductors, thermoelectric power S is proportional to the energy derivative of the density of electronic states. In low-dimensional (nanostructured) systems the density of electronic states has sharp peaks and theoretically a high thermopower.

Based on the Seebeck effect found in 1821, Seebeck voltage V is proportional to the temperature difference ΔT and Seebeck coefficient S (also thermopower) [21];

$$S = \frac{V}{T} \quad (1)$$

The Seebeck coefficient for semiconductors is typically of the order of 100 μ V/K [22]. Conversely, this

process can operate in reverse to make TE cooler (the Peltier effect). In P-type semiconductors, S is a positive value (negative in N-type semiconductor). In the fabrication of a TEG, both N-type and P-type are applied to achieve a larger potential difference. For metals and degenerate semiconductors, the Seebeck coefficient is defined as [23],

$$S = \frac{8\pi^2 k_B^2}{3e h^2} m T \left(\frac{\pi}{3N_s} \right)^{\frac{2}{3}} \quad (2)$$

where N_s is the charge carrier concentration, m is the effective mass of the charge carrier, h is the Planck's constant, k_B is the Boltzmann constant, and e is the carrier charge. S is strongly influenced by the charge carrier energy distribution, and in particular it increases when the average difference between the carrier energies and the Fermi energy increases [24].

In addition, We consider separately the electron diffusion S_{diff} and phonon drag, S_{drag} contribution to the thermopower $S = S_{diff} + S_{drag}$ for the Si nanowire over the temperature T from 50 K to 400K [25]. Charge carriers dissipate heat to the lattice through a process that first involves momentum conserving (non-dissipative) electron-phonon collisions. The phonons that contribute to phonon drag cannot have a wavelength shorter than λ_{min} which is determined by the size of the Fermi surface. Phonon drag is observed in metals only at low temperature because the Fermi surface is large and the heat carrying short-wavelength phonons have short lifetime at lower temperature ($T < 20$ K). Umklapp (non-momentum-conserving) phonon-phonon scattering processes determine the rate of phonon heat dissipation. The Debye energy θ_D sets the energy scale for umklapp scattering. The number of umklapp phonons available to dissipate long wavelength phonons is given by Bose-Einstein function

$$N_{ph} = \frac{1}{\exp\left(\frac{\theta_D}{T}\right) - 1} \quad (3)$$

Leading to a scattering rate, $\frac{1}{\tau_{ph}} \propto N_{ph}$, when $T \gg \theta_D$, so that $\frac{1}{\tau_{ph}} \propto T$ because $\theta_D = 640$ K for Silicon, the Bose-Einstein expression must be applied for $T \leq 350$ K. The electronic contribution S_{diff} is estimated using Mott formula;

$$S_{diff}(T) = \frac{\pi^2 k_B^2 T}{3e} \left(\frac{\partial \ln \sigma(E)}{\partial E} \right) \quad (4)$$

where the conductivity derivative equals the reciprocal of the energy scale over which it varies.

For $T > 200$ K, the experimental thermopower data of silicon nanowire fit to the theoretical expression,

$$S = S_{diff} + S_{drag}$$

$$S = aT + b \left[\exp\left(\frac{\theta_D}{T}\right) - 1 \right] \quad (5)$$

where a , b and θ_D are varied to obtain the best fit to experimentally observed data [26].

III. RESULTS AND DISCUSSION

Like Si NWs, SiGe alloy NWs exhibited excellent enhancement as a result of the phonon boundary scattering. Individual P-type SiGe alloy NW was reported with thermal conductivity $1.1 \text{ W m}^{-1} \text{ K}^{-1}$ and Figure of Merit (ZT) 0.18 at 300K experimentally [27]. In a typical TE modeling of SiGe NWs, the optimized ZT is 1.3 at 800K for the $\text{Si}_{0.73}\text{Ge}_{0.27}$ NW with 26 nm diameter where the ionized impurity concentration should be about $1.0 \times 10^{20} \text{ cm}^{-3}$ [28]. In principle, the ZT of SiGe at different temperatures can be further enhanced by the diameter reduction and doping concentration optimization. The reduction in SiGe alloy NWs came from the phonon alloy scattering which scatters short wavelength phonons with high frequency, while low frequency phonons are scattered by the phonon boundary scattering.

Diameter (D) and length of SiGe NWs are also important issues for the TE properties [29]. The thin NWs show a reduction of thermal conductivity when compared with the thick ones. A thorough study has been designed to find the certain trend [30] and the result is that thermal conductivity is proportional to D when D is small. However, this dependence becomes continually weaker with increasing D. Combined with the Ge constituent effect, the group found the linear trend slowed down with a higher Ge content, up to $x = 0.5$. The same situation happens with the increasing Si in Ge. This is because of the coexistence of alloy and boundary scattering. SiGe NW arrays with a longer length exhibit a higher Seebeck coefficient while the thermal conductivity decreases with increasing Ge concentration and NW length.

When it comes to doping type, N-type SiGe NWs are reported to have remarkably higher ZT and power factor compared to P-type SiGe NWs at 300K (Shi et al., 2010). With a cross section area of 2.3 nm^2 , the ZT of N-type

$\text{Si}_{1-x}\text{Ge}_x$ NWs was theoretically calculated to be 4.3 [31]. In [32] Noroozi et al. the peak of Seebeck coefficient for N-type and P-type $\text{Si}_{0.53}\text{Ge}_{0.47}$ are 8 and 1.8 mV/K at 315K, which can be explained by the temperature dependence of the interaction of defects. With the same diffusion process applied, the carrier mobility in N-type SiGe NWs is higher than P-type, which results in a much higher Seebeck coefficient in N-type SiGe NWs than P-type. Also, the measured maximum power factor of N-type is two times higher than P-type.

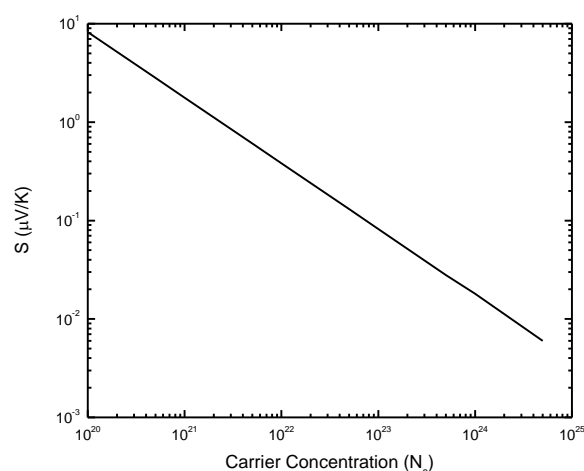


Fig.1: Variation of Thermopower S with Carrier Concentration (N_s)

Figure 1 show our calculations from equation (2) wherein it is observed that, as the carrier concentration decreases with thermopower S .

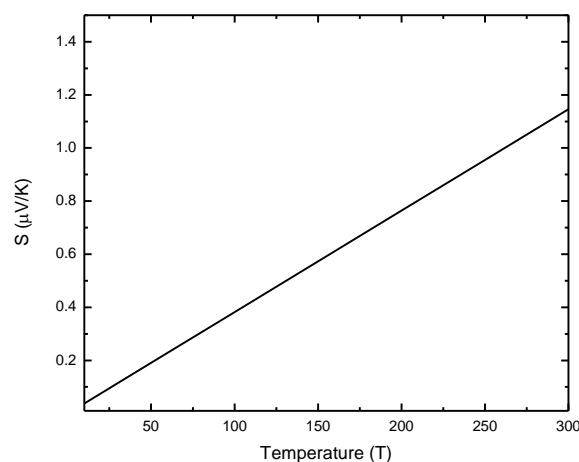


Fig.2: Variation of Thermopower S with Temperature (T).

Figure 2 is the variation of thermopower with absolute carrier temperature from equation (2). It is observed that, thermopower S varies linearly with temperature T .

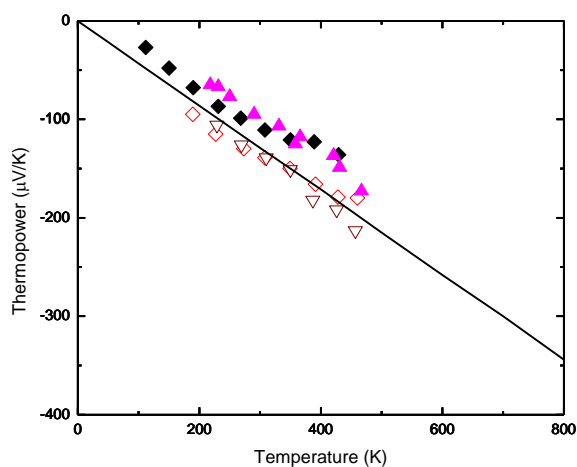


Fig.3: Comparison of experimental thermopower S with theory. Different symbols show experimental observations (26) and straight line is our theoretical data.

In Figure 3, to obtain a best fit, α , b and θ_D are used as adjustable parameters in equation (5). In our calculations, Since for lower temperature $T < 200$ K, the contribution towards thermopower is only due to electron diffusion thermopower. With the adjustable parameter α , we will not observe best with the experimental data. So we used adjustable parameter $\alpha = 2.0 \mu\text{V/K}$ to obtain a best fit in figure 3 for the entire temperature range. This is good agreement with predicted linear temperature dependence for $k_B T$ less than Fermi energy, which is about 200 meV agreeing with Mott formula and experimental results. Figure 3 shows comparison between calculated thermopower with experimental observations [26]. Our calculations are in good agreement with the experimental results. The symbols of different colors in figure 3 are for thermopower of different diameters mentioned in ref [26].

IV. CONCLUSION

Semiconductors are the most important materials in our modern technology-based world. In the last three decades, semiconductor nanostructures have become one of the more rapidly developing area within the nanoscience research community. Among the different semiconductor nanostructures, SiGe nanowires, that can be manipulated through size reduction, geometry variation and alloying,

are considered one of the key developments for next generation technologies, due to their ease processing, unique properties and compatibility with the existent silicon based microelectronics industry. In this theoretical work, we have discussed the major dependence of thermopower with carrier concentration and electron temperature. Also we compared the available experimental data with our theoretical calculations and obtained good agreement for SiGe nanowires.

REFERENCES

- [1] Radousky, H. B., and Liang, H. (2012). *Nanotechnology* **23**:502001.
- [2] Yan, J., Liao, X., Yan, D., and Chen, Y. (2018). *J. Microelectromech. Syst.* **27**, 1–18.
- [3] Gadea, G., Pacios, M., Morata, Á., and Tarancón, A. (2018b). *J. Phys. D Appl. Phys.* **51**:423001.
- [4] Radamson, H., Zhang, Y., He, X., Cui, H., Li, J., Xiang, J., et al. (2017). *Appl. Sci.* **7**:1047
- [5] Kim, J., Shim, W., and Lee, W. (2015). *J. Mater. Chem. C* **3**, 11999–12013.
- [6] Li, D., Wu, Y., Kim, P., Shi, L., Yang, P., and Majumdar, A. (2003b). *Appl. Phys. Lett.* **83**, 2934
- [7] Takabatake, T., Suekuni, K., Nakayama, T., and Kaneshita, E. (2014). *Rev. Mod. Phys.* **86**, 669
- [8] Rogl, G., Grytsiv, A., Rogl, P., Peranio, N., Bauer, E., Zehetbauer, M., et al (2014) *Acta Mater.* **63**, 30
- [9] Ishibe, T., Tomeda, A., Watanabe, K., Kamakura, Y., Mori, N., Naruse, N., et al, (2018). *ACS Appl. Mater. Interfaces* **10**, 37709
- [10] Goldsmid, H. J. (2014). *Materials* **7**, 2577
- [11] Zeier, W. G., Schmitt, J., Hautier, G., Aydemir, U., Gibbs, Z. M., Felser, C et al, (2016). *Nat. Rev Mater.* **1**:16032.
- [12] Ni, W. X., Ekberg, J. O., Joelsson, K. B., Radamson, H. H., Henry, A., Shen G D, et al. (1995). *J. Cryst. Growth.* **157**, 285
- [13] Dresselhaus, M. S., Chen, G., Tang, M. Y., Yang, R. G., Lee, H., Wang, D. Z., et al (2007). *Adv. Mater.* **19**, 1043–1053.
- [14] Gadea, G., Pacios, M., Morata, Á., and Tarancón, A. (2018b). *J. Phys. D Appl. Phys.* **51**:423001.
- [15] Akbari-Saatlu, M., Procek, M., Mattsson, C., Thungstrom, G., Nilsson, H. E. Xiong et al. (2020). *Nanomaterials* **10**:2215.
- [16] Calaza, C., Salleras, M., Dávila, D., Tarancón, A., Morata, A., Santos, J. D., et al (2015). *Mater. Today Proc.* **2**, 675
- [17] Wolfsteller, A., Geyer, N., Nguyen-Duc, T. K., Das Kanungo, P., Zakharov, N. D., Reiche, M., et al. (2010). *Thin Solid Films.* **518**, 2555
- [18] Liu, Y., Zhang, M., Ji, A., Yang, F., and Wang, X. (2016). *RSC Adv.* **6**, 48933–48961.
- [19] Grauby, S., Puyoo, E., Rampnoux, J.-M., Rouvière, E., and Dilhaire, S. (2013) *J. Phys. Chem. C* **117**, 9025
- [20] Haras, M., and Skotnicki, T. (2018). *Nano Energy* **54**, 461
- [21] Gadea, G., Morata, A., and Tarancón, A. (2018). *Semiconduct. Semimetals* **98**, 321

- [22] Goktas, N. I., Wilson, P., Ghukasyan, A., Wagner, D., McNamee, S., and LaPierre, R. R. (2018). *Appl. Phys. Rev.* **5**:041305.
- [23] Snyder, G. J., and Toberer, E. S. (2008). *Nat. Mater.* **7**, 105
- [24] Pennelli, G. (2014). *Beilstein J. Nanotechnol.* **5**, 1268
- [25] Kasala Suresha, (2022), *Int. J. Chem. Maths. Phys.* **6**, 01
- [26] M Amato, M Palummo, R Rurali and S Ossidini, (2013), *Chem. Rev.* **114**
- [27] Martinez, J. A., Provencio, P. P., Picraux, S. T., Sullivan, J. P., and Swartzentruber, B. S. (2011). *J. Appl. Phys.* **110**:074317
- [28] Yi, S.-I., and Yu, C. (2015). *J. Appl. Phys.* **117**:035105.
- [29] Wang, Z., and Mingo, N. (2010). *Appl. Phys. Lett.* **97**:101903.
- [30] Shi, L., Yao, D., Zhang, G., and Li, B. (2009). *Appl. Phys. Lett.* **95**:063102.
- [31] Shi, L., Yao, D., Zhang, G., and Li, B. (2010). *Appl. Phys. Lett.* **96**:173108.
- [32] Noroozi, M., Hamawandi, B., Jayakumar, G., Zahmatkesh, K., Radamson, H. H., and Toprak, M. S. (2017). *J. Nanosci. Nanotechnol.* **17**, 1622